Dynamical properties of layered superionic conductors

T. Tomoyose and K. Yonashiro
Department of Physics, Division of General Education, Ryukyu University, Nishihara, Okinawa 903-01, Japan

M. Kobayashi
Department of Physics, Niigata University, Ikarashi, Niigata 950-21, Japan

(Received 20 July 1989; revised manuscript received 1 February 1990)

A model layered superionic conductor, which is composed of alternating layers of superionic conductors and ionic crystal, is described on the basis of a continuum model. Using linear-response theory, the dielectric function and ionic conductivity of the system are obtained as a function of frequency, wave number, and the distance between the adjacent layers. It is shown that these response functions satisfy a sum rule. The longitudinal collective modes obtained from the dielectric function are classified into two kinds of modes: the acoustic-phonon mode and the coupled optical-phonon–ionic-plasma mode. The ionic-plasma mode has changed from the three-dimensional to the two-dimensional plasma mode with the increase of the distance between layers. Also in the strong-coupling limit where the distance is small enough the ionic-plasma mode has shown two phases: bulklike and acousticlike plasma modes.

I. INTRODUCTION

One of the current interests in the field of crystal-growth physics is to explore the possibility of artificial substances such as semiconductor superlattices. Recent advances made in molecular-beam expitaxy have made possible the growth of ultrathin layers with thicknesses on the order of atomic dimensions.[1] Today we can study various new materials with superlattice structure which are composed of alternating layers of different materials. In particular, type-I (e.g., $GaAs/Al_xGa_{1-x}As$) and type-II (e.g., InAs/GaSb) semiconductor superlattices have been extensively studied. If electrons occupy only the lowest subband in a type-I semiconductor superlattice, we can treat the type-I semiconductor superlattice as a layered electron gas (LEG).

The collective excitations in LEG have attracted much interest.[2–10] It is well known that the energy of two-dimensional (2D) plasmons is proportional to the square root of the wave number in the long-wavelength limit,[11] while that of three-dimensional (3D) plasmons is constant, independent of wave number.[12] On the other hand, plasmons of LEG systems change their dispersion relation from 2D-plasmon-like to 3D-plasmon-like with decreasing distance between layers.[13] This dimensional crossover property of plasma modes is a common characteristic of any layered system of charged particles.

One proposed superlattice is composed of alternating layers of superionic conductors (SIC's) and ionic crystals. We call it the layered SIC (LSIC). Because of the layered structure in the LSIC system, the dispersion relation of plasma modes will also be expected to change from 2D-like to 3D-like with decreasing distance between layers as in the LEG system. Hence the collective modes of LSIC are expected to be different from that of the usual 3D SIC system.

SIC's are widely known as solid electrolytes with a high ionic conductivity comparable to that of a liquid electrolyte. Collective modes of 3D SIC have been investigated by many authors.[14–19] Kobayashi *et al.*[19] discussed the coupled modes of plasmons and longitudinal optical phonons in silver chalcogenides. Jäckle[16] predicted that under the influence of the Coulomb force the ionic diffusion mode is converted into a relaxation mode in the long-wavelength limit. The electric field induced by ionic density fluctuations has no effect on elastic waves, but has a quantitative effect on damped optical phonons and changes completely the character of the diffusion mode. This indicates that the Coulomb field has a strong influence on the coupling of plasma modes and other collective modes. In the LSIC system, however, plasma modes change their dispersion relations depending on the distance between layers as described above. This structure dependence of plasma modes presumably affects the dispersion relations of the coupled modes in the LSIC system.

In the present paper, using the continuum model, we investigate longitudinal collective excitations and the dynamical properties of the LSIC system. The main purpose of the present paper is to study the dynamical difference between the LSIC and 3D SIC systems.

Our model structure is shown in Fig. 1. The system consists of an infinite array of parallel SIC layers a distance d apart. The space between SIC layers is filled with an ionic crystal with the static dielectric constant ϵ_0. Here the ionic crystal is regarded as a background medium which does not affect the dynamical properties of the SIC layers. We assume that the SIC layer is sufficiently thin and may be treated as a 2D SIC plane. As an actual system, we consider a LSIC system composed of 2D α-AgI planes separated by LiCl ionic crystal. From the continuum model, the crystalline cage composed of lattice ions (I^-) is assumed to be immersed in a viscous fluid of mobile ions (Ag^+). The relative motion of two ionic components is governed by the short-range visocelastic force with a memory effect and the the long-range Coulomb force. Ionic dynamics in the LSIC are described by the equations of motion for each kind of ion and the Maxwell equation. A current density in a SIC plane is induced by the relative motion between ions, producing an effective electric field which affects the ionic motion in neighboring planes. Thus these equations have to be solved self-consistently.

The outline of the present paper is as follows. In Sec. II we present the equations of motion using the continuum model. In Sec. III we describe the dielectric function and the ionic conductivity of the LSIC system on the basis of linear-response theory. We find that these response functions satisfy a sum rule. In Sec. IV we present the dispersion relations of the longitudinal collective modes. In Sec. V we calculate numerically the interplane distance dependence and the frequency dependence of ionic conductivity. In the final section we summarize and discuss our results.

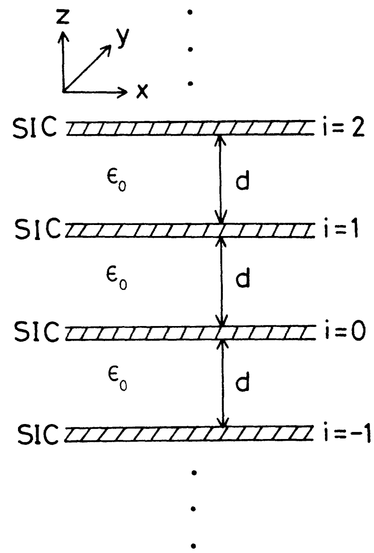

FIG. 1. The system of infinite-layered superionic conductors. 2D SIC planes parallel to the x-y plane are arranged with regular intervals d. The space between the planes is filled with an ionic crystal of dielectric constant ϵ_0.

II. EQUATIONS OF MOTION

As in shown in Fig. 1, we take the z axis to be perpendicular to the SIC planes and denote the coordinate in the x-y plane by the position vector $\mathbf{r}$. The SIC planes are located at $z=z_i$, where $z_i=id$ ($i=0,\pm1,\pm2,\ldots$).

The dynamics of the lattice ions is described by the lattice displacement field in the crystalline cage. The equation of motion for the 2D lattice displacement field $\xi_i(\mathbf{r},t)$ in the ith SIC plane is given by[18]

$$\frac{\partial^2}{\partial t^2}\xi_i(\mathbf{r},t)-\left[V_L^2+\Gamma_L\frac{\partial}{\partial t}\right]\nabla\nabla\cdot\xi_i(\mathbf{r},t)+\frac{1}{m_1}\int_{-\infty}^{t}dt'\,M(t-t')\left[\frac{\partial}{\partial t'}\xi_i(\mathbf{r},t')-\mathbf{v}_i(\mathbf{r},t')\right]=-\frac{q}{m_1}\mathbf{E}_t(\mathbf{r},z_i,t)\ , \tag{2.1}$$

with $M(t)=m^*\omega_0^2\exp(-t/\tau)$ and $(m^*)^{-1}=m_1^{-1}+m_2^{-1}$. Here, m_1 and m_2 are the anion (I^-) and cation (Ag^+) masses, respectively; q is the elementary electronic charge, V_L is the longitudinal sound velocity, and Γ_L its phenomenological damping coefficient; ω_0 is the optical frequency with a relaxation time τ in a relative ionic motion. The field $\mathbf{v}_i(\mathbf{r},t)$ is the 2D velocity field of mobile ions in the ith SIC plane and $\mathbf{E}_t(\mathbf{r},z,t)$ is the tangential component of the total electric field $\mathbf{E}(\mathbf{r},z,t)$ at the point $(\mathbf{r},z)$.

The motion of mobile ions is treated as that of a viscous fluid. It can be described by the 2D velocity field $\mathbf{v}_i(\mathbf{r},t)$ and the dimensionless density fluctuation $n_i(\mathbf{r},t)$. Here, $n_i(\mathbf{r},t)$ is defined by $n_i(\mathbf{r},t)=[N_i(\mathbf{r},t)-N_0]/N_0$, where $N_i(\mathbf{r},t)$ is the 2D number density of mobile ions and N_0 is its average value. The linearized hydrodynamic equations for these fields are given by

$$\frac{\partial}{\partial t}n_i(\mathbf{r},t)+\nabla\cdot\mathbf{v}_i(\mathbf{r},t)=0\ , \tag{2.2a}$$

$$\frac{\partial}{\partial t}\mathbf{v}_i(\mathbf{r},t)+c_0^2\nabla n_i(\mathbf{r},t)-\alpha_L\nabla^2\mathbf{v}_i(\mathbf{r},t)+\frac{1}{m_2}\int_{-\infty}^{t}dt'\,M(t-t')\left[\mathbf{v}_i(\mathbf{r},t')-\frac{\partial}{\partial t'}\xi_i(\mathbf{r},t')\right]=\frac{q}{m_2}\mathbf{E}_t(\mathbf{r},z_i,t)\ , \tag{2.2b}$$

where c_0 is the sound velocity in the fluid composed of mobile ions and α_L is the viscosity.

The 2D Fourier transforms of Eqs. (2.1) and (2.2) give us the following equations:

$$\dot{\xi}_i(\mathbf{k},\omega)=-\frac{iq\omega[\omega^2-c_0^2(\omega)k^2]}{m_1H(k,\omega)}\mathbf{E}_t(\mathbf{k},z_i,\omega)\ , \tag{2.3a}$$

$$\mathbf{v}_i(\mathbf{k},\omega)=\frac{iq\omega[\omega^2-V_L^2(\omega)k^2]}{m_2H(k,\omega)}\mathbf{E}_t(\mathbf{k},z_i,\omega)\ , \tag{2.3b}$$

where $\mathbf{k}$ is a 2D wave vector in the x-y plane and ω is the frequency. Here the functions $G(k,\omega)$ and $H(k,\omega)$ are defined as

$$G(k,\omega)=[\omega^2-V_s^2(\omega)k^2]\ , \tag{2.4a}$$

$$H(k,\omega)=[\omega^2-V_L^2(\omega)k^2][\omega^2-c_0^2(\omega)k^2]-\Omega_0^2(\omega)[\omega^2-V_s^2(\omega)k^2]\ , \tag{2.4b}$$

where

$$V_s^2(\omega)=[m_1V_L^2(\omega)+m_2c_0^2(\omega)]/(m_1+m_2)\ ,$$

$$V_L^2(\omega)=(V_L^2-i\omega\Gamma_L)\ ,$$

and

$$c_0^2(\omega)=(c_0^2-i\omega\alpha_L)\ .$$

The frequency Ω_0 corresponds to that of the damped optical phonon in the SIC system:

$$\Omega_0^2(\omega)=-i\omega\int_0^\infty dt\, e^{i\omega t}M(t)/m^*=\omega_0^2\omega/(\omega+i/\tau)\ . \tag{2.5}$$

The 2D current density $\mathbf{j}_i(\mathbf{r},t)$ in the ith SIC plane combines with the relative motion of ions through the equation $\mathbf{j}_i(\mathbf{r},t)=N_0q[\mathbf{v}_i(\mathbf{r},t)-\dot{\xi}_i(\mathbf{r},t)]$, where $\dot{\xi}_i\equiv(\partial/\partial t)\xi_i$. Then, from Eq. (2.3), the Fourier component is given by

$$\mathbf{j}_i(\mathbf{k},\omega)=\frac{iN_0q^2\omega G(k,\omega)}{m^*H(k,\omega)}\mathbf{E}_t(\mathbf{k},z_i,\omega)\ . \tag{2.6}$$

III. DIELECTRIC RESPONSE AND IONIC CONDUCTIVITY

A. Dielectric function

We calculate here the dielectric function of LSIC on the basis of the linear-response theory.[20] A weak external charge $\rho_{\rm ex}(\mathbf{r},z,t)$ induces a charge fluctuation $\rho_{\rm in}(\mathbf{r},z,t)$ in the system. The total electric field $\mathbf{E}(\mathbf{r},z,t)$ and the electric displacement $\mathbf{D}(\mathbf{r},z,t)$ in the system obey the following equations:

$$\nabla\cdot\mathbf{E}(\mathbf{r},z,t)=4\pi\rho_{\rm tot}(\mathbf{r},z,t)=4\pi[\rho_{\rm in}(\mathbf{r},z,t)+\rho_{\rm ex}(\mathbf{r},z,t)]\ , \tag{3.1}$$

$$\nabla\cdot\mathbf{D}(\mathbf{r},z,t)=4\pi\rho_{\rm ex}(\mathbf{r},z,t)\ , \tag{3.2}$$

where $\rho_{\rm tot}(\mathbf{r},z,t)$ is the total charge. Taking the Fourier transforms of Eqs. (3.1) and (3.2), we obtain the formula for the longitudinal dielectric function of the LSIC system as follows:

$$\epsilon_L(\mathbf{k},k_z,\omega)=\frac{\rho_{\rm ex}(\mathbf{k},k_z,\omega)}{\rho_{\rm tot}(\mathbf{k},k_z,\omega)}=1-\frac{\mathbf{k}\cdot\mathbf{E}_{\rm in}(\mathbf{k},k_z,\omega)}{\mathbf{k}\cdot\mathbf{E}(\mathbf{k},k_z,\omega)}\ , \tag{3.3}$$

where $\mathbf{E}_{\rm in}(\mathbf{k},k_z,\omega)$ is the electric field induced in the system and k_z is the wave number perpendicular to the planes.

In order to obtain the dielectric function, we have to calculate the induced field $\mathbf{E}_{\rm in}(\mathbf{k},k_z,\omega)$. We can obtain it by summing the induced fields caused by all SIC planes. The electric field $\mathbf{E}_{\rm in}^{(0)}(\mathbf{r},z,t)$ produced by the current on the 0th SIC plane satisfies the following Maxwell equation:

$$\nabla^2\mathbf{E}_{\rm in}^{(0)}(\mathbf{r},z,t)-\nabla\nabla\cdot\mathbf{E}_{\rm in}^{(0)}(\mathbf{r},z,t)-\frac{\epsilon_0}{c^2}\frac{\partial^2}{\partial t^2}\mathbf{E}_{\rm in}^{(0)}(\mathbf{r},z,t)=\frac{4\pi}{c^2}\frac{\partial}{\partial t}\mathbf{j}_0(\mathbf{r},t)\delta(z)\ , \tag{3.4}$$

where c is the velocity of light, and $\delta(z)$ is Dirac's δ function. Using the 2D Fourier transform, we obtain the solution of Eq. (3.4):

$$\mathbf{E}_{\rm in}^{(0)}(\mathbf{k},z,\omega)=\begin{bmatrix}\mathbf{E}_t^{(0)}(\mathbf{k}\omega)\exp(-\beta|z|)\\ \pm i\mathbf{k}\cdot\mathbf{E}_t^{(0)}(\mathbf{k},\omega)\exp(-\beta|z|)/\beta\end{bmatrix} \tag{3.5}$$

where $\mathbf{E}_t^{(0)}$ is the tangential and $\pm i\mathbf{k}\cdot\mathbf{E}_t^{(0)}/\beta$ the z components of the induced electric field at $z=0$, and $\beta=(k^2-\epsilon_0\omega^2/c^2)^{1/2}$.

Taking the contribution from all SIC planes, the tangential component of the total induced field $\mathbf{E}_{{\rm in},t}(\mathbf{k},z,\omega)$ is obtained as follows:

$$\mathbf{E}_{{\rm in},t}(\mathbf{k},z,\omega)=\mathbf{E}_{{\rm in},t}^{(0)}(\mathbf{k},z,\omega)F(\beta,k_z)\ , \tag{3.6}$$

where $F(\beta,k_z)=\sinh\beta d/(\cosh\beta d-\cos k_zd)$. $F(\beta,k_z)$ is the structure factor which characterizes the layered system.

Furthermore, the tangential component of Eq. (3.5) at $z=0$ leads to the relation

$$\mathbf{E}_{{\rm in},t}^{(0)}(\mathbf{k},z=0,\omega)+\frac{2i\pi\beta}{\epsilon_0\omega}\mathbf{j}_0(\mathbf{k},\omega)=0\ . \tag{3.7}$$

By combining Eqs. (2.6), (3.6), and (3.7), we get the relation between the induced electric field $\mathbf{E}_{\rm in}(\mathbf{k},z,\omega)$ and the total electric field $\mathbf{E}(\mathbf{k},z,\omega)$:

$$\mathbf{E}_{{\rm in},t}(\mathbf{k},z,\omega)=\frac{2\pi\beta N_0q^2G(k,\omega)}{\epsilon_0m^*H(k,\omega)}F(\beta,k_z)\mathbf{E}_t(\mathbf{k},z,\omega)\ . \tag{3.8}$$

From Eqs. (3.3) and (3.8), we get the longitudinal dielectric function of the LSIC system:

$$\epsilon_L(\mathbf{k},k_z,\omega)=1-\omega_p^2(\beta,k_z)G(k,\omega)/H(k,\omega)\ , \tag{3.9}$$

where $\omega_p(\beta,k_z)$ gives plasma frequency of the LSIC system. In the nonretarded limit ($\beta\to k$), we get $\omega_p^2(k,k_z)=\Omega_{2p}^2(k)F(k,k_z)$ where $\Omega_{2p}(k)$ denotes the 2D ionic plasma frequency given by $\Omega_{2p}(k)=(2\pi N_0q^2k/m^*\epsilon_0)^{1/2}$.

B. Ionic conductivity

We now calculate the ionic conductivity of the LSIC system. Since there is no charge transfer between SIC planes, the ionic conductivity tensor has nonzero elements only in the x-y plane. Therefore the ionic conductivity $\sigma(\mathbf{k},k_z,\omega)$ is defined by

$$\mathbf{j}_{\rm in}(\mathbf{k},k_z,\omega)=\sigma(\mathbf{k}k_z,\omega)\mathbf{E}_t(\mathbf{k},k_z,\omega)\ , \tag{3.10}$$

where the induced current density $\mathbf{j}_{\rm in}(\mathbf{r},z,t)$ is given by

$$\mathbf{j}_{\text{in}}(\mathbf{r},z,t)=\sum_i \mathbf{j}_i(\mathbf{r},t)\delta(z-z_i) . \tag{3.11}$$

Under an external current, the total electric field obeys the following Maxwell equation:

$$\begin{aligned}\nabla^2\mathbf{E}(\mathbf{r},z,t)-\nabla\nabla\cdot\mathbf{E}(\mathbf{r},z,t)-\frac{\epsilon_0}{c^2}\frac{\partial^2}{\partial t^2}\mathbf{E}(\mathbf{r},z,t)\\ =\frac{4\pi}{c^2}\frac{\partial}{\partial t}\mathbf{j}_{\text{tot}}(\mathbf{r},z,t)\\ =\frac{4\pi}{c^2}\frac{\partial}{\partial t}[\mathbf{j}_{\text{in}}(\mathbf{r},z,t)+\mathbf{j}_{\text{ex}}(\mathbf{r},z,t)] ,\end{aligned} \tag{3.12}$$

where $\mathbf{j}_{\text{tot}}(\mathbf{r},z,t)$ and $\mathbf{j}_{\text{ex}}(\mathbf{r},z,t)$ are the total and external current density. Each current density satisfies the continuity equation and is assumed to be 2D flows confined to the SIC planes. Thus the Maxwell equation (3.12) can be analytically solved. After carrying out the Fourier transform for Eq. (3.12), we can write the z and tangential components of it as

$$k_z\mathbf{k}\cdot\mathbf{E}_t(\mathbf{k},k_z,\omega)-\beta^2E_z(\mathbf{k},k_z,\omega)=0 , \tag{3.13a}$$

$$\begin{aligned}(k_z^2+\beta^2)\mathbf{E}_t(\mathbf{k},k_z,\omega)-\mathbf{k}\mathbf{k}\cdot\mathbf{E}_t(\mathbf{k},k_z,\omega)\\ -\mathbf{k}k_zE_z(\mathbf{k},k_z,\omega)=\frac{i4\pi\omega}{c^2}\mathbf{j}_{\text{tot}}(\mathbf{k},k_z,\omega) .\end{aligned} \tag{3.13b}$$

Since we restrict our attention to the longitudinal modes ($\mathbf{k}\|\mathbf{E}_t$ and $\mathbf{k}\|\mathbf{j}_{\text{tot}}$), we can simplify the notation by $\mathbf{k}\mathbf{k}\cdot\mathbf{E}_t=k^2\mathbf{E}_t$. A combination of Eqs. (3.13a) and (3.13b) thus leads to

$$\mathbf{E}_t(\mathbf{k},k_z,\omega)=-\frac{i4\pi\beta^2}{\epsilon_0\omega(\beta^2+k_z^2)}\mathbf{j}_{\text{tot}}(\mathbf{k},k_z,\omega) . \tag{3.14}$$

Substituting Eq. (3.14) into Eq. (3.10), we obtain the longitudinal ionic conductivity

$$\sigma_L(\mathbf{k},k_z,\omega)=\frac{i\epsilon_0\omega(\beta^2+k_z^2)\mathbf{k}\cdot\mathbf{j}_{\text{in}}(\mathbf{k},k_z,\omega)}{4\pi\beta^2\mathbf{k}\cdot\mathbf{j}_{\text{tot}}(\mathbf{k},k_z,\omega)} . \tag{3.15}$$

Taking account of the continuity equation, we can express Eq. (3.15) in terms of the ratio $\rho_{\text{ex}}/\rho_{\text{tot}}$ which defines the dielectric function in Eq. (3.3). Then the ionic conductivity is related to the dielectric function in the following form:

$$\sigma_L(\mathbf{k},k_z,\omega)=\frac{i\epsilon_0\omega}{4\pi}\frac{\beta^2+k_z^2}{\beta^2}[1-\epsilon_L(\mathbf{k},k_z,\omega)] . \tag{3.16}$$

C. Sum rules of response functions

We will show that the response functions satisfy a sum rule. First we investigate the sum rule for the longitudinal dielectric function $\epsilon_L(\mathbf{k},k_z,\omega)$. From Eq. (3.9), the sum rule for the imaginary part of $\epsilon_L(\mathbf{k},k_z,\omega)$ is expressed as

$$\begin{aligned}\int_{-\infty}^{\infty}\omega\,\text{Im}\epsilon_L(\mathbf{k},k_z,\omega)\frac{d\omega}{\pi}\\ =-\omega_p^2(k,k_z)\,\text{Im}\int_{-\infty}^{\infty}\frac{g(k,\omega)}{\prod_{j=1}^{5}(\omega-\omega_j)}\frac{d\omega}{\pi} ,\end{aligned} \tag{3.17}$$

where $g(k,\omega)=\omega(\omega+i/\tau)G(k,\omega)$, and the frequencies ω_j are the solutions of $(\omega+i/\tau)H(k,\omega)=0$.

We can evaluate the integral in Eq. (3.17) by using a contour integral. The result obtained is as follows:

$$\begin{aligned}\int_{-\infty}^{\infty}\omega\,\text{Im}\epsilon_L(\mathbf{k},k_z,\omega)\frac{d\omega}{\pi}\\ =\omega_p^2(k,k_z)\left[2\,\text{Re}\sum_{i=1}^{4}\frac{g(k,\omega_i)}{\prod_{j=1\,(j\neq i)}^{4}(\omega_i-\omega_j)}-1\right] .\end{aligned} \tag{3.18}$$

The residue theorem leads to

$$\text{Re}\sum_{i=1}^{4}g(k,\omega_i)\Big/\prod_{j=1\,(j\neq i)}^{4}(\omega_i-\omega_j)=1$$

so that Eq. (3.18) is reduced to

$$\int_{-\infty}^{\infty}\omega\,\text{Im}\epsilon_L(\mathbf{k},k_z,\omega)\frac{d\omega}{\pi}=\omega_p^2(k,k_z) . \tag{3.19}$$

In the strong-coupling limit ($kd \ll 1$), there are two different cases to consider: $k_z=0$ and $k_zd=\pi$. When $k_z=0$ and $F(k,k_z)\simeq 2/kd$, we get

$$\int_{-\infty}^{\infty}\omega\,\text{Im}\epsilon_L(\mathbf{k},k_z,\omega)\frac{d\omega}{\pi}=\Omega_p^2=\left[\frac{4\pi n_{\text{eff}}q^2}{m^*\epsilon_0}\right] , \tag{3.20}$$

where Ω_p denotes an effective 3D ionic plasma mode with an effective 3D ionic density, $n_{\text{eff}}=N_0/d$. In this case, Eq. (3.20) leads to the sum rule in the 3D system.

For the case of $k_zd=\pi$, taking account of $F(\mathbf{k},k_z)\simeq kd/2$, we obtain another expression of the sum rule:

$$\int_{-\infty}^{\infty}\omega\,\text{Im}\epsilon_L(\mathbf{k},k_z,\omega)\frac{d\omega}{\pi}=\Omega_{\text{AP}}^2(k)=\left[\frac{\pi N_0q^2d}{m^*\epsilon_0}\right]k^2 , \tag{3.21}$$

where $\Omega_{\text{AP}}(k)$ is an ion–acoustic-plasma frequency. Equation (3.21) is characteristic of the layered system.

In the weak-coupling limit ($kd \gg 1$), the effect of the layered structure vanishes because $F(k,k_z)=1$. Hence all planes are independent of each other and then the sum rule is reduced to that of an isolated single layer:

$$\int_{-\infty}^{\infty}\omega\,\text{Im}\epsilon_L(\mathbf{k},k_z,\omega)\frac{d\omega}{\pi}=\Omega_{2p}^2(k) . \tag{3.22}$$

We can also obtain a sum rule for ionic conductivity. Replacing $\omega\,\text{Im}\epsilon_L$ in Eq. (3.19) by $\text{Re}\sigma_L$ in Eq. (3.16), we get

$$\int_{-\infty}^{\infty}\text{Re}\sigma_L(\mathbf{k},k_z,\omega)\frac{d\omega}{\pi}=\frac{\epsilon_0}{4\pi}\frac{(kd)^2+(k_zd)^2}{(kd)^2}\omega_p^2(k,k_z) . \tag{3.23}$$

In the strong-coupling limit ($kd \ll 1$, $k_zd \ll 1$), Eq. (3.23) represents the sum rule of the 3D system:

$$\int_{-\infty}^{\infty}\text{Re}\sigma_L(\mathbf{k},k_z,\omega)\frac{d\omega}{\pi}=\epsilon_0\Omega_p^2/4\pi . \tag{3.24}$$

In the weak-coupling limit ($kd \gg 1$, $k_z d \gg 1$), the sum rule is given by

$$\int_{-\infty}^{\infty} \mathrm{Re}\sigma_L(\mathbf{k},k_z,\omega)\frac{d\omega}{\pi} = \epsilon_0 \Omega_{2p}^2(k)/4\pi \ , \qquad (3.25)$$

which corresponds to that of the 2D system.

IV. COLLECTIVE MODES

A. Dispersion relation

In this section we calculate the dispersion relation of collective modes in the system. In the following we consider only the case of the nonretarded limit ($\beta \to k$). As is well known, the dispersion relations of longitudinal collective modes are derived from $\epsilon_L(\mathbf{k},k_z,\omega)=0$, i.e., $1=\omega_p^2(k,k_z)G(k,\omega)/H(k,\omega)$. Taking account of Eq. (2.4), we obtain the equation for ω:

$$[\omega^2 - V_L^2(\omega)k^2][\omega^2 - c_0^2(\omega)k^2] - \Omega_0^2(\omega)[\omega^2 - V_s^2(\omega)k^2] = \omega_p^2(k,k_z)[\omega^2 - V_s^2(\omega)k^2] \ . \qquad (4.1)$$

This equation is factorized as $[\omega^2-\omega_+^2(\omega)][\omega^2-\omega_-^2(\omega)]=0$, where $\omega_\pm(\omega)$ is defined as

$$\omega_\pm^2(\omega) = \tfrac{1}{2}(\Omega_+^2 + V_+^2 k^2) \pm \tfrac{1}{2}[(\Omega_+^2 + V_+^2 k^2)^2 - 4\Omega_+^2 V_s^2(\omega)k^2 - 4V_L^2(\omega)c_0^2(\omega)k^4]^{1/2} \ , \qquad (4.2)$$

with $\Omega_+^2 = \Omega_0^2(\omega) + \omega_p^2(k,k_z)$ and $V_+^2 = V_L^2(\omega) + c_0^2(\omega)$. The functions $\omega_+(\omega)$ and $\omega_-(\omega)$ are related to an upper and a lower collective mode of the system, respectively.

Because the continuum model is valid in the long-wavelength region, we will consider the collective modes only in the long-wavelength limit ($k \to 0$). The upper mode satisfies the dispersion relation $\omega^2 = \lim_{k\to 0}\omega_+^2(\omega) = \Omega_0^2(\omega) + \omega_p^2(k,k_z) + O(k^2)$. This is identical to the third degree equation for ω [note that $\Omega_0^2(\omega) = \omega_0^2\omega/(\omega + i/\tau)$]:

$$\omega^3 + i\omega^2/\tau - \omega[\omega_0^2 + \omega_p^2(k,k_z)] - i\omega_p^2(k,k_z)/\tau = 0 \ , \qquad (4.3)$$

which represents the coupled optical-phonon–plasma mode.

On the other hand, the lower mode satisfies the dispersion relation of $\omega^2 = \lim_{k\to 0}\omega_-^2(\omega) = V_s^2(\omega)k^2$. Then we get the damped acoustic-phonon mode of $\omega_- = \pm Vk - i\Gamma k^2$, with $V = [(m_1 V_L^2 + m_2 c_0^2)/(m_1+m_2)]^{1/2}$ and $\Gamma = (m_1\Gamma_L + m_2\alpha_L)/2(m_1+m_2)$. These acoustic waves are caused by the in-phase motion of two ionic components on a SIC plane. This motion does not induce charge-density fluctuation and so does not couple to the electric field.

B. Strong-coupling limit ($kd \ll 1$)

In the LSIC system, the dispersion relations of the coupled modes with the plasma mode depend on the correlation between SIC planes through the structure factor $F(k,k_z)$ contained in the plasma mode $\omega_p^2(k,k_z)$. In the strong-coupling limit ($kd \ll 1$), we consider two cases of $k_z=0$ and $k_z \neq 0$ for describing the collective excitations in the LSIC system.

1. Upper modes

First we consider the upper mode for the case of $k_z=0$. When $kd \ll 1$ and $k_z=0$, the plasma mode in Eq. (4.3) becomes the effective 3D ionic plasma mode. The physical origin of the effective 3D plasma mode is evident. When the ionic densities in all SIC planes oscillate in phase ($k_z=0$) in the z direction, it is hard to distinguish a 3D plasma mode propagating in the $\mathbf{k}$ direction from the effective 3D plasma mode.

In the long-wavelength limit ($k \to 0$), taking account of the condition $\Omega_p^2/\omega_0^3\tau \ll 1$ (for AgI, $\omega_0 \sim 105$ cm^{-1}, $\tau^{-1} \sim 15.6$ cm^{-1}, and $\Omega_p < \omega_0$),[16,21] we can expand Eq. (4.3) as a series in powers of $\Omega_p^2/\omega_0^3\tau$. Then we obtain the following high-frequency upper modes within the first order of $\Omega_p^2/\omega_0^3\tau$:

$$\omega_+ = \pm(\omega_0^2 + \Omega_p^2 - 1/4\tau^2)^{1/2} - \frac{i}{2\tau}\frac{\omega_0^2 + s_0/2\tau}{\omega_0^2 + \Omega_p^2 + s_0/2\tau} \ , \qquad (4.4)$$

with $s_0 = -1/2\tau \pm i(\omega_0^2 + \Omega_p^2 - 1/4\tau^2)^{1/2}$. This high-frequency upper mode represents the coupled mode of optical phonons and 3D plasmons. On the other hand, the low-frequency upper mode is purely imaginary:

$$\omega_{\mathrm{rel}} = -i\Omega_p^2/(\omega_0^2 + \Omega_p^2)\tau \ , \qquad (4.5)$$

which corresponds to the relaxation mode. From Eq. (4.5) we find that the relaxation mode corresponds to a combined mode of the effective 3D plasma mode Ω_p and the optical mode ω_0. This situation is similar to that in the 3D SIC system where the relaxation mode is interpreted as the overdamped plasma mode connected with the relative viscous flow of two ionic components.[16]

For the case of $k_z \neq 0$ and $kd \ll 1$, the plasma mode turns to an acousticlike mode given by $\omega_p(k,k_z) = \Omega_{\mathrm{AP}}(k)/\sin(k_z d/2)$. This mode is due to the characteristics of the layered system of charged particles.[8–10,22] Olego *et al.*[13] have succeeded in observing the acoustic plasmon (AP) in GaAs-$\mathrm{Al}_x\mathrm{Ga}_{1-x}$As by inelastic light scattering.

The acoustic plasmon has also been found by Pinczuk *et al.*[23] in the 3D electron-hole system by the same method as that used by Olego *et al.* This mode has been theoretically predicted by Pines and Schrieffer[24] and Harrison.[25] The acoustic plasma mode of the 3D electron-hole system differs from that of the layered system in physical origin. The acoustic plasmons in the 3D system can be excited by two kinds of carriers with a different mass ratio. On the other hand, in the layered system containing only a single type of carrier, the acoustic plasma mode can exist only through the effect of the layered structure. Thus the excitation mechanisms for the acoustic plasma mode are essentially different between these systems.

In the long-wavelength limit ($k \to 0$), the acoustic plasma mode is considerably smaller than the optical mode so that the coupling between them can be ignored. For the case of $k_z \neq 0$, the long-wavelength upper mode satisfies

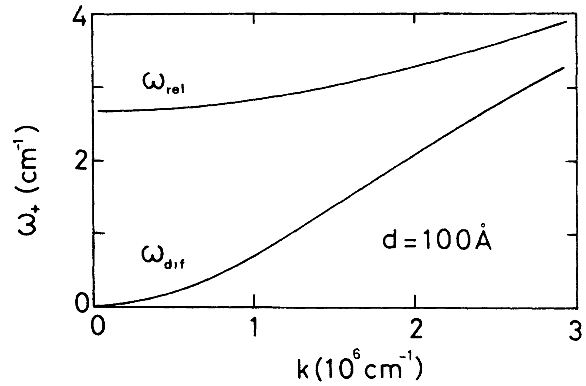

FIG. 2. Dispersion relations of low-frequency upper modes. The absolute values of the frequencies are plotted as a function of a wave number k for the two cases, $k_z d=0$ and $k_z d=\pi$. In the strong-coupling limit ($kd \ll 1$), the former case leads to the relaxation mode $\omega_{\rm rel}$ given by Eq. (4.5), and the latter leads to the diffusion mode $\omega_{\rm dif}$ given by the second term of Eq. (4.7).

the dispersion relation $\omega^2=\Omega_0^2(\omega)$, i.e.,

$$\omega_+=\pm(\omega_0^2-1/4\tau^2)^{1/2}-\frac{i}{2\tau}\ , \tag{4.6}$$

which represents damped longitudinal optical phonons.

Contrary to the effective 3D case ($k_z=0$), in the present case of $k_z\neq 0$ we can see that the low-frequency upper mode is transformed from the relaxation mode into a diffusion mode. This is discussed in the next subsection.

2. *Diffusion modes*

The relaxation mode, as discussed in the preceding subsection, disappears and is transformed into the diffusion mode in the case of $k_z\neq 0$. In this case, charge densities on adjacent planes oscillate out of phase in the z direction so that they make little contribution to the total electric field. This reduction of Coulomb force causes a softening of the effective 3D plasma mode. Hence the relaxation mode, connected with the plasma mode, changes into a diffusionlike mode which is proportional to k^2. The diffusion mode is determined from the term of order k^4 in the wave-number expansion of Eq. (4.1) and satisfies the dispersion relation $\omega_+^2(\omega)\omega_-^2(\omega)=0$ within $0(k^4)$. Taking account of Eq. (4.2), we get

$$[\Omega_0^2(\omega)+\omega_p^2(k,k_z)]V_s^2(\omega)k^2+V_L^2(\omega)c_0^2(\omega)k^4=0\ .$$

This leads to the diffusion mode up to $O(k^2)$:

$$\omega_{\rm dif}=-i[V_L^2c_0^2k^2/V_s^2+\Omega_{\rm AP}^2(k)]/\omega_0^2\tau\ . \tag{4.7}$$

The first term denotes the intrinsic diffusion term in the absence of the Coulomb field and the second is due to the softening of the plasma mode.

In Fig. 2 we have plotted the absolute values of the low-frequency upper modes given by Eq. (4.3) as a function of wave number k. We have used the physical parameters of α-AgI as those of SIC planes in our numerical calculation. The values of these parameters are shown in Table I. In Table I, the value of the relaxation time τ is taken such that the experimental value of about 2 $(\Omega\,{\rm cm})^{-1}$ for the dc ionic conductivity of α-AgI is obtained. The value of N_0 is determined from the limiting condition that the AgI SIC layers, when arrayed with a separation equal to the lattice constant (5.07 Å), must be equivalent to the 3D AgI system. The diffusion mode $\omega_{\rm dif}$ and the relaxation mode $\omega_{\rm rel}$ correspond to the cases of $k_z d=\pi$ and $k_z d=0$, respectively. In the strong-coupling limit ($kd\ll 1$), the relaxation mode is derived from Eq. (4.5) and the diffusion mode corresponds to the second term of Eq. (4.7).

TABLE I. Values of numerical parameters of α-AgI and LiCl. We have taken a typical value of 10^5 cm^{-1} for $|\mathbf{k}|$.

Physical parameters of α-AgI	
N_0: 2D average number density	8.11×10^{14} cm^{-2}
m_1: mass of I^- ion	2.11×10^{-22} g
m_2: mass of Ag^+ ion	1.79×10^{-22} g
τ: viscoelastic relaxation time	$\tau^{-1}=15.6$ cm^{-1}
ω_0: oscillator frequency	105 cm^{-1}
V_L: longitudinal sound velocity (cage)	$V_Lk=0.8$ cm^{-1}
c_0: sound velocity (fluid)	$c_0k=0.2$ cm^{-1}
Γ_L: longitudinal damping coefficient	$\Gamma_Lk^2=0.1V_Lk$
α_L: longitudinal viscosity	5×10^{-12} cm^{-1}
Physical parameters of LiCl	
ϵ_0: static dielectric constant of LiCl	12

C. Weak- ($kd\gg 1$) and intermediate- ($kd\sim 1$) coupling case

When $kd\gg 1$ and $F(k,k_z)\simeq 1$, the plasma mode is given by the 2D plasma frequency and the long-wavelength upper mode satisfies the dispersion relation $\omega^2=\Omega_0^2(\omega)+\Omega_{2p}^2(k)+O(k^2)$. This is identical to the third degree equation for ω:

$$\omega^3+i\omega^2/\tau-\omega[\omega_0^2+\Omega_{2p}^2(k)]-i\Omega_{2p}^2(k)/\tau=0\ . \tag{4.8}$$

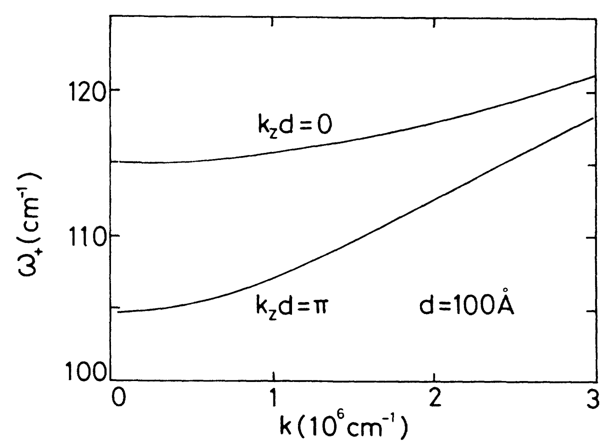

FIG. 3. Dispersion relations of the high-frequency upper mode ω_+ given by Eq. (4.3). For the case $k_zd=0$, ω_+ denotes the coupled mode of optical phonons and 3D plasma modes given by Eq. (4.4) in the strong-coupling limit ($kd\ll 1$). For the case $k_zd=\pi$, ω_+ represents the damped optical phonons given by Eq. (4.6).

Since the condition $\Omega_{2p}^2(k)=\Omega_p^2 kd/2 \gg \Omega_p^2$ is fulfilled in the weak-coupling limit ($kd \gg 1$), we cannot neglect the last term in Eq. (4.8). In this case the upper mode is rather complicated and we should calculate it numerically.

For an intermediate situation of $kd \simeq 1$, we can expand Eq. (4.3) in powers of $\omega_p^2(k,k_z)/\omega_0^3\tau$. Taking account of the relation $\omega_p^2(k,k_z)=\Omega_p^2 F(k,k_z)kd/2$, within the lowest order of $\omega_p^2(k,k_z)/\omega_0^3\tau$ we find

$$\omega_+ = \pm[\omega_0^2+\omega_p^2(k,k_z)-1/4\tau^2]^{1/2}-i/2\tau \ , \qquad (4.9)$$

which represents the coupled modes of plasma modes and optical-phonon modes in the intermediate coupling case.

Figure 3 shows the dispersion relations of the high-frequency upper modes given by Eq. (4.3). From Fig. 3 we find that the upper modes ω_+ split into two modes in the strong-coupling limit ($kd \ll 1$): one of these ($k_z d=0$) is the coupled mode of 3D ionic plasmons and optical phonons, and the other ($k_z d=\pi$) is the damped optical-phonon mode. In the intermediate coupling region the upper modes are represented by Eq. (4.9) and approach a degenerate mode independent of k_z in an isolated single layer.

V. NUMERICAL CALCULATION OF IONIC CONDUCTIVITY

A. Interplane distance dependence of conductivity

We calculate numerically the ionic conductivity given by Eq. (3.16) as a function of the distance d between SIC planes. The values of parameters used in the calculation are shown in Table I. The calculated results are shown in Fig. 4. The solid curve shows the calculated results and the dashed line indicates the value at $d=\infty$, namely the 2D ionic conductivity.

From Fig. 4, we see a dimensional crossover of the conductivity, from 3D to 2D. In the limit of $d=\infty$, the ionic conductivity tends to that of the isolated 2D SIC layer and is independent of the layered structure. On the other hand, in the limit of $d=0$ the ionic conductivity has to agree with that of the 3D SIC system. Reσ in Fig. 4, however, diverges at $d=0$. This behavior is clarified by the following explanation: we have used layers of zero thickness instead of finite thickness, and treated them as 2D planes with an ionic number density N_0. In this case, the effective 3D number density $n_{\text{eff}}=N_0/d$ shows a divergence at $d=0$. This corresponds to the unrealistic situation where we can array closely a vast number of layers in any narrow space. If we take into account the thickness of each SIC layer, it is possible to remove the divergence at $d=0$.

However, the dynamical description for the microscopic region of small d is beyond the range of application of our model. Thus we have to limit our discussion to values of d sufficiently larger than the lattice constant of SIC.

From Fig. 4 we see that the 2D ionic conductivity is fairly large. If we make a LSIC system from SIC slabs with a number density of $N_0 \sim 10^{15}$ cm^{-2} by molecular-beam epitaxy, it will have a high ionic conductivity comparable to that of a 3D SIC system. By changing the superlattice period of the LSIC, we can prepare a range of LSIC samples for studying the dimensional crossover behavior of the ionic conductivity.

B. Frequency dependence of conductivity

We will now calculate numerically the frequency-dependent ionic conductivity of the LSIC composed of α-AgI planes and discuss it in detail. In Figs. 5 and 6 the real part of $\sigma_L(\mathbf{k},k_z,\omega)$ is plotted as a function of frequency ω. In Fig. 5, Re$\sigma_L(\mathbf{k},k_z,\omega)$ has a broad peak at about 100 cm^{-1}, which is nearly equal to the frequency of the optical mode ω_0. This suggests that the broad peak is related to an ionic motion connected with optical modes. Also, Fig. 6 shows a dip at about 0.37 cm^{-1}, which corresponds to the frequency of acoustic modes having the k value used in the present computation. This characteristic ω dependence can be well explained from the point of view of ionic motion in a SIC plane.

First we discuss the dip in Fig. 6. By using the velocity field ratio $\mathbf{v}_i(\mathbf{k},\omega)/\boldsymbol{\xi}_i(\mathbf{k},\omega)$, we rewrite the 2D ionic

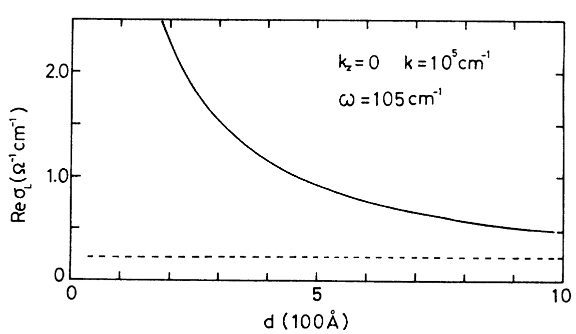

FIG. 4. Interplane distance dependence of the ionic conductivity Re$\sigma_L(k,k_z,\omega)$ for the LSIC composed of α-AgI planes. The parameter values used in the present computation are shown in Table I. The solid curve represents the ionic conductivity calculated from Eq. (3.16). The dashed line indicates the 2D ionic conductivity in the limit of $d=\infty$.

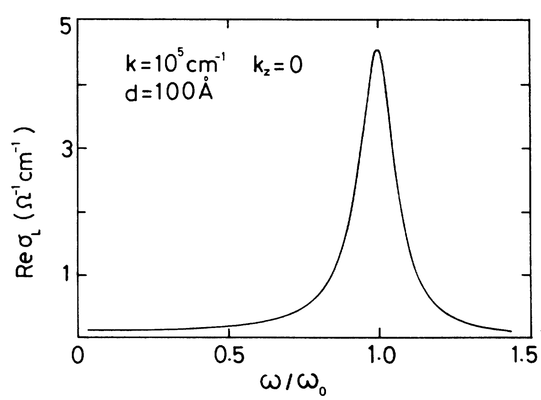

FIG. 5. Frequency dependence of the real part of ionic conductivity Re$\sigma_L(k,k_z,\omega)$ in the high-frequency range. The parameter values used are shown in Table I. The broad peak has a maximum at about $\omega=100$ cm^{-1}.

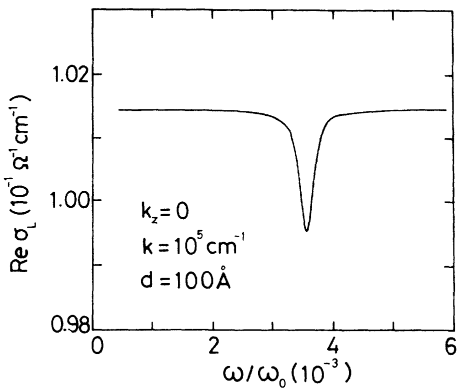

FIG. 6. Frequency dependence of the conductivity $\mathrm{Re}\sigma_L(k,k_z,\omega)$ in the low-frequency range. $\mathrm{Re}\sigma_L$ shows a dip at $\omega=0.37\ \mathrm{cm}^{-1}$. This value of ω is equal to that of the acoustic mode with the k value used in the present computation.

current density in the form

$$\mathbf{j}_i(\mathbf{k},\omega)=-N_0 q\dot{\xi}_i(\mathbf{k},\omega)[1-\mathbf{v}_i(\mathbf{k},\omega)/\dot{\xi}_i(\mathbf{k},\omega)] \ . \tag{5.1}$$

Taking account of Eq. (2.3), we get the following ratio for acoustic modes:

$$\left[\frac{\mathbf{v}_i(\mathbf{k},\omega)}{\dot{\xi}_i(\mathbf{k},\omega)}\right]_{\text{acoust}}=-\frac{m_1}{m_2}\left[\frac{m_2(c_0^2-V_L^2)k^2+O(k^3)}{m_1(V_L^2-c_0^2)k^2+O(k^3)}\right]=1 \ . \tag{5.2}$$

Substituting Eq. (5.2) into Eq. (5.1), we find that the current density vanishes. This indicates that anions and cations oscillate in phase and cannot yield any net charge density. Thus the acoustic mode does not contribute to the total induced current of Eq. (3.11). For these reasons, at the acoustic mode frequency the ionic conductivity rapidly decreases and causes the dip in the ω dependence.

Next we consider the broad peak in the spectrum of ionic conductivity shown in Fig. 5. For the optical modes of Eqs. (4.4) and (4.6), we get the following velocity ratio:

$$\left[\frac{\mathbf{v}_i(\mathbf{k},\omega)}{\dot{\xi}_i(\mathbf{k},\omega)}\right]_{\text{opt}}=-\frac{m_1}{m_2}\left[\frac{\omega_+^2+O(k^2)}{\omega_+^2+O(k^2)}\right]=-\frac{m_1}{m_2} \ . \tag{5.3}$$

In this case, we find that the center of mass is fixed. Hence the optical modes correspond to the out-of-phase motion of two ionic components on the ith SIC plane. Substituting Eq. (5.3) into Eq. (5.1), we obtain

$$\mathbf{j}_i(\mathbf{k},\omega)=-N_0 q\dot{\xi}_i(\mathbf{k},\omega)(1+m_1/m_2) \ , \tag{5.4}$$

which produces a finite current flow on the ith plane. Thus the relative ionic motions on all SIC planes contribute to the total current at the optical frequency.

We will now show that the ionic conductivity in Eq. (3.16) has a maximum at about $\omega_0=105\ \mathrm{cm}^{-1}$. Using Eqs. (2.4) and (3.9), we calculate $\mathrm{Re}\sigma_L(\mathbf{k},k_z,\omega)$ in the long-wavelength limit ($k\to 0$). The result obtained is as follows:

$$\mathrm{Re}\sigma_L(\omega)=\frac{\sigma_0\omega_0^4}{[\omega^2-(\omega_0^2-1/2\tau^2)]^2+(\omega_0^2/\tau^2-1/4\tau^4)} \ , \tag{5.5}$$

where σ_0 denotes the dc ionic conductivity of $\sigma_0=n_{\text{eff}}q^2/m^*\omega_0^2\tau$ in the LSIC system. We find that $\mathrm{Re}\sigma$ in Eq. (5.5) has a maximum at $\omega_{\max}$ given by $\omega_{\max}=(\omega_0^2-1/2\tau^2)^{1/2}$. The frequency $\omega_{\max}$ is nearly equal to that of the optical mode of Eqs. (4.4) and (4.6). The broadening of the spectrum depends on the relaxation time τ of the relative ionic motion. The spectral peak gets sharper with increasing τ.

VI. DISCUSSION AND CONCLUSION

In the present paper we have studied theoretically the collective excitations and the dynamical properties of layered superionic conductors (LSIC). We have found that the collective modes are classified into two kinds of mode, the lower mode and the upper mode. The lower mode corresponds to the acoustic-phonon mode, while the low-frequency and the high-frequency upper mode correspond to the relaxation mode and the coupled optical-phonon–ionic-plasma mode, respectively.

The LSIC dispersion relations of ionic-plasma modes are strongly related to the layered structure of the system. The plasma modes show various regimes in their dispersion relations depending on the distance and the correlation between SIC planes. In the strong-coupling limit ($kd\ll 1$), the LSIC system is essentially a 3D-like system, except for the appearence of the acoustic plasma modes due to the out-of-phase correlation between SIC layers. In the weak-coupling limit ($kd\gg 1$), we found that the plasma frequency ω_p of the LSIC is proportional to $k^{1/2}$. In an intermediate situation, $kd\simeq 1$, ω_p is proportional to $[kF(k,k_z)]^{1/2}$, which shows an intermediate character between 2D and 3D systems. This dispersion relation is the same as that in the layered electron gas (LEG) system. The structure factor $F(k,k_z)$ reflects a characteristic of the layered structure in LSIC.

In the strong-coupling situation, there are two branches of the plasma modes, a 3D plasma mode and acoustic plasma modes. For the case of $k_z=0$, ionic densities on all SIC planes oscillate together in phase in the z direction, and thus lead to an effective 3D plasma oscillation in the system. Even in the long-wavelength limit, the 3D plasma mode strongly couples with the optical phonons on all planes and forms a coupled mode of optical phonons and the 3D ionic plasma mode. For the case of $k_z\neq 0$, the plasma mode changes into an acousticlike mode. The acoustic plasma mode has a frequency proportional to k in the long-wavelength limit. This is due to a softening of the plasma mode, because charge densities oscillating out of phase ($k_z\neq 0$) on different planes cause a decrease of their restoring force, i.e., a reduction of the Coulomb field. In the long-wavelength limit, the acoustic plasma mode is so small that the coupling with optical phonons is ignored, hence damped optical phonons outlive it. However, the acoustic plasma mode strongly influences the characteristic of the relaxation mode. Under the reduction of the Coulomb field, the relaxation mode is converted into a diffusionlike mode due to the softening of the plasma mode. This behavior exhibits a striking contrast to that in the 3D bulk SIC system and is characteristic of the LSIC system.

The lower mode does not correspond to the coupled optical-phonon plasma mode but represents an acoustic-phonon mode. The Coulomb field caused by the ionic charge-density fluctuation has no effect on the acoustic-phonon modes. This physical meaning is evident. The acoustic-phonon mode corresponds to the in-phase oscillation of the ions on any SIC plane so that it cannot couple to the ionic charge-density fluctuation oscillating out of phase.

We have also calculated the sum rules for the dielectric function and the conductivity. The expression for the sum rule is closely related to the correlation between layers. In the strong-coupling limit ($kd \ll 1$), there are two expressions. For the case of in-phase correlation ($k_z d = 0$) the sum rule gives the usual 3D expression. On the other hand, the out-of-phase correlation ($k_z d = \pi$) leads to an expression described by the acoustic plasma modes. In the weak-coupling limit ($kd \gg 1$), the sum rule obtained represents that of a 2D system. Our derivation of the expression for the sum rule seems to be the first for a layered system of charged particles.

We have numerically calculated the frequency and distance dependence of ionic conductivity for an LSIC composed of α-AgI planes. The frequency dependence of the conductivity is found to be similar to that of bulk α-AgI. The broad peak and the dip structure in the spectrum are attributed to the optical-phonon modes and the acoustic-phonon modes, respectively. This behavior in the spectrum is similar to that in 3D SIC. On the other hand, the value of the ionic conductivity changes from a 3D to a 2D value with increasing distance between SIC planes. The distance dependence enables us to see a dimensional crossover in ionic conductivity of the LSIC system. Calculation using our model gives the 2D ionic conductivity in the limit of infinitely separated planes, but does not converge to the 3D ionic conductivity value for smaller values of d. This theoretical discrepancy will disappear if one uses an improved LSIC model, i.e., by taking account of the thickness of each SIC layer. Recently, the fast ion conductor superlattice was studied by Aniya and Kobayashi[26] taking into consideration the finite layer thickness.

Before finishing our discussions, we will consider some remaining problems connected with the present theory. Our theory of the continuum model is restricted within the macroscopic description. The dynamics of atomic motion at the interface between the SIC and ionic crystal has not been sufficiently studied. In a description of the atomic motion at the interface, the effect of the microscopic structure is expected to be important. Thus we may need some microscopic description such as a hopping model. In general, the atomic motion in SIC ought to be considered as a many-body problem. Several theoretical treatments from this point of view have been presented in explaining atomic diffusion in SIC. Yokota[27] and Okazaki[28,29] suggested that the individual atomic motion in SIC is a strongly correlated diffusion process, such as a caterpillar mechanism.[27] However, we also believe that the continuum model is fairly useful for studying the collective behavior of complicated atomic motion in SIC.

ACKNOWLEDGMENTS

This work is partially supported by a Grant-in-Aid for Scientific Research from the Ministry of Education, Science and Culture of Japan.

[1] *Molecular Beam Epitaxy and Heterostructures,* edited by L. L. Chang and K. Ploog (Nijhoff, Boston, 1985).
[2] P. B. Visscher and L. M. Falicov, Phys. Rev. B **3**, 2541 (1971).
[3] A. L. Fetter, Ann. Phys. (N.Y.) **88**, 1 (1974).
[4] M. Kobayashi, J. Mizuno, and I. Yokota, J. Phys. Soc. Jpn. **39**, 18 (1975).
[5] M. Apostol, Z. Phys. B **22**, 13 (1975).
[6] A. Caille, M. Banville, and M. J. Zuckermann, Solid State Commun. **24**, 805 (1977).
[7] G. F. Giuliani and J. J. Quinn, Phys. Rev. Lett. **51**, 919 (1983).
[8] S. Das Sarma and J. J. Quinn, Phys. Rev. B **25**, 7603 (1982).
[9] W. L. Bloss and E. M. Brody, Solid State Commum. **43**, 523 (1982).
[10] A. C. Tselis and J. J. Quinn, Phys. Rev. B **29**, 3318 (1984).
[11] F. Stern, Phys. Rev. Lett. **18**, 546 (1967).
[12] C. Kittel, *Introduction to Solid State Physics* (Wiley, New York, 1986), Chap. 10.
[13] D. Olego, A. Pinczuk, A. C. Gossard, and W. Wiegmann, Phys. Rev. B **25**, 7867 (1982).
[14] B. A. Huberman and R. M. Martin, Phys. Rev. B **13**, 1498 (1976).
[15] K. R. Subbaswamy, Solid State Commun. **19**, 1157 (1976).
[16] J. Jäckle, Z. Phys. B **30**, 255 (1978).
[17] H. Hayashi, M. Kobayashi, and I. Yokota, Solid State Commun. **31**, 847 (1979).
[18] N. Mizoguchi, H. Hayashi, M. Kobayashi, and I. Yokota, J. Phys. Soc. Jpn. **50**, 2043 (1981).
[19] M. Kobayashi, F. Sukegawa, and I. Yokota, Solid State Ion. **2**, 237 (1981).
[20] D. Pines, *Elementary Excitations in Solids* (Benjamin, New York, 1964), Chap. 3.
[21] P. Brüesch, S. Strassler, and H. R. Zeller, Phys. Status Solidi A **31**, 217 (1975).
[22] T. Takahashi and M. Kobayashi, Solid State Commun. **56**, 485 (1985).
[23] A. Pinczuk, J. Shah, and P. A. Wolff, Phys. Rev. Lett. **47**, 1487 (1981).
[24] D. Pines and J. R. Schrieffer, Phys. Rev. **124**, 1387 (1961).
[25] M. J. Harrison, J. Phys. Chem. Solids **23**, 1079 (1962).
[26] M. Aniya and M. Kobayashi, Appl. Phys. A **49** (1989).
[27] I. Yokota, J. Phys. Soc. Jpn. **21**, 420 (1966).
[28] H. Okazaki, J. Phys. Soc. Jpn. **23**, 355 (1967).
[29] H. Okazaki, J. Phys. Soc. Jpn. **43**, 213 (1977).